



HAL
open science

A thioredoxin-mimetic peptide exerts potent anti-inflammatory, antioxidant, and atheroprotective effects in ApoE2.Ki mice fed high fat diet

Fanny Canesi, Véronique Mateo, Dominique Couchie, Sonia Karabina, Anne Nègre-Salvayre, Mustapha Rouis, Khadija El Hadri

► **To cite this version:**

Fanny Canesi, Véronique Mateo, Dominique Couchie, Sonia Karabina, Anne Nègre-Salvayre, et al.. A thioredoxin-mimetic peptide exerts potent anti-inflammatory, antioxidant, and atheroprotective effects in ApoE2.Ki mice fed high fat diet. *Cardiovascular Research*, 2019, 115 (2), pp.292-301. 10.1093/cvr/cvy183 . inserm-03978156

HAL Id: inserm-03978156

<https://inserm.hal.science/inserm-03978156>

Submitted on 8 Feb 2023

HAL is a multi-disciplinary open access archive for the deposit and dissemination of scientific research documents, whether they are published or not. The documents may come from teaching and research institutions in France or abroad, or from public or private research centers.

L'archive ouverte pluridisciplinaire **HAL**, est destinée au dépôt et à la diffusion de documents scientifiques de niveau recherche, publiés ou non, émanant des établissements d'enseignement et de recherche français ou étrangers, des laboratoires publics ou privés.

A thioredoxin-mimetic peptide exerts potent anti-inflammatory, antioxidant, and atheroprotective effects in ApoE2.Ki mice fed high fat diet

Fanny Canesi¹, Véronique Mateo², Dominique Couchie¹, Sonia Karabina³, Anne Nègre-Salvayre⁴, Mustapha Rouis^{1†}, and Khadija El Hadri^{1*†}

¹Sorbonne Université, Institut de Biologie Paris Seine (IBPS), CNRS, INSERM ERL U-1164, Biological Adaptation and Ageing (B2A), UMR-8256, F-75252, Paris, France; ²Sorbonne Université, INSERM U-1135, CIMI-Paris, Hôpital Pitié-Salpêtrière Centre de recherche d'Immunologie et Maladies infectieuses, UMRS CR7, F-75013, Paris, France; ³Sorbonne Université, INSERM, Hôpital Armand-Trousseau, Physiopathologie Des Maladies Genétiques D'Expression Pédiatrique, UMR_S933, F-75012, Paris, France; and ⁴Institut des Maladies Métaboliques et Cardiovasculaires, INSERM-UPS, Lipides, Peroxydation, Signalisation et Maladies Vasculaires, UMR 1048, F-31432, Toulouse, France

Received 2 October 2017; revised 30 March 2018; editorial decision 5 July 2018; accepted 10 July 2018; online publish-ahead-of-print 13 July 2018

Time for primary review: 40 days

Aims

Oxidative stress and inflammation play a pathogenic role in atherosclerosis. Thioredoxin-1 (Trx-1) is an anti-oxidative, anti-inflammatory protein with atheroprotective effects. However, *in vivo* cleavage of Trx-1 generates a truncated pro-inflammatory protein, Trx-80, which compromises the therapeutic use of Trx-1. Here we analysed whether the thioredoxin-mimetic peptide (TxMP), CB3 might exert anti-oxidative, anti-inflammatory, and atheroprotective effects in ApoE2.Ki mice.

Methods and results

We synthesized a small TxMP, Ac-Cys-Pro-Cys-amide, CB3 and characterized its antioxidant and anti-inflammatory effects on cultured peritoneal murine macrophages. CB3 significantly and dose-dependently reduced the level of reactive oxygen species in lipopolysaccharides (LPS)-activated macrophages. In addition, it efficiently lowered LPS-induced inflammatory process through NF- κ B inhibition, as evidenced by the reduced secretion of monocyte chemoattractant protein-1, interleukin (IL)-1 β , IL-6, and tumor necrosis factor (TNF)- α by macrophages. Nevertheless, CB3 did not affect cholesterol accumulation in macrophages. A daily-administered dose of 10 μ g/g body weight CB3 to ApoE2.Ki mice on high fat diet did not affect plasma of total cholesterol and triglycerides levels but significantly reduced the plasma levels of pro-inflammatory cytokines (IL-33 and TNF- α) and oxidative markers. In contrast, it significantly induced the plasma levels of anti-inflammatory proteins (adiponectin, IL-10). In addition, CB3 reduced the number of pro-inflammatory M1 macrophages in spleen and decreased the ratio of M1/M2 macrophages in atherosclerotic lesion areas. Finally, CB3 significantly reduced the surface area of aortic lesions.

Conclusions

Our results clearly showed that similar to the full length Trx-1, CB3 exerts protective effects, by reducing inflammation and oxidative stress in macrophages and in ApoE2.Ki mice. The atheroprotective effect of CB3 opens promising therapeutic approaches for treatment of atherosclerosis.

Keywords

Atherosclerosis • Thioredoxin-1 • Inflammation • Oxidative stress • Macrophages • Thioredoxin-mimetic peptide • CB3

1. Introduction

Cardiovascular diseases (CVD) remain the leading cause of morbidity and death worldwide.¹ The majority of CVD results from complications

of atherosclerosis which is characterized by a state of unresolved low-grade inflammation of the arterial wall. The inflammatory process plays a key role in all stages of atherosclerosis.² A crucial step of the atherogenic process is the infiltration of monocytes into the subendothelial

* Corresponding author. Tel: 33 1 44 27 20 28; fax: 33 1 44 27 51 40, E-mail: khadija.zegouagh@upmc.fr

† The last two authors contributed equally to the study.

space of arteries and their subsequent differentiation into resident macrophages within the atherosclerotic lesions.³ An important feature of macrophages is their plasticity and ability to adopt diverse activation states in response to their microenvironment.⁴ For many years macrophages have been classified into two main groups, representing the extremes of a continuum, namely 'classically activated' or M1 and 'alternatively activated' or M2 macrophages.^{5–7} Upon stimulation with interferon- γ (IFN- γ), and toll-like receptor (TLR) ligands, such as lipopolysaccharides (LPS), macrophages adopt a pronounced pro-inflammatory M1 phenotype, characterized by the secretion of pro-inflammatory cytokines, reactive oxygen species (ROS), and nitrogen intermediates.^{3,8} Conversely, interleukin (IL)-4, IL-13,⁶ peroxisome proliferator-activated receptor γ (PPAR- γ) activators,⁹ and adiponectin¹⁰ polarize macrophages towards an anti-inflammatory M2 phenotype. While M1 macrophages possess bactericidal and inflammatory activity, M2 macrophages are involved in tissue remodelling, immunosuppression, and show phagocytic activity.³

Increasing evidence suggests that risk factors for CVD can lead to dramatic increase in the concentration of ROS in the vascular wall. When the rate of ROS production exceeds the capacity of the antioxidant defence system, oxidative stress occurs which contributes to endothelium damage, oxidized low-density lipoproteins (oxLDL) generation, and stimulation of atherosclerotic mediators leading to atherosclerosis.¹¹ Thioredoxin-1 (Trx-1), a highly conserved 12-kDa protein, plays a vital role in maintaining the intracellular homeostatic redox state by keeping cysteine residues reduced in cells.¹² Trx-1 functions by the reversible oxidation of two Trx-specific redox-active cysteine residues (Cys-32 and Cys-35) to form a disulfide bond that, in turn, can be reduced by the action of Trx reductase (TrxR) and dihydronicotinamide adenine dinucleotide phosphate (NADPH).¹² It has become clear that Trx-1 protects against CVD through its anti-oxidative and anti-inflammatory capacities, its specific interaction with several proteins and through its capacity to modify gene expression.¹² Thus, over expression of human Trx-1 in mice attenuated focal ischaemic brain damage and increased the resistance to various oxidative stresses leading to longer survival compared to control mice.¹³ Furthermore, exogenous Trx-1 exerts distinct cytoprotective effects after transient cerebral ischaemia in mice by means of its redox-regulating activity.¹⁴ Recently, we have demonstrated that Trx-1 promoted the polarization of macrophages into an anti-inflammatory M2 phenotype and significantly reduced the LPS-induced polarization of macrophages toward inflammatory M1 phenotype. These results may explain its protective effects in CVDs in animal models.¹⁵ Indeed, Trx-1 administered to hyperlipoproteinaemic ApoE2.Ki mice shifted the phenotype pattern of lesional macrophages to predominantly M2 over M1, and the aortic lesion area was significantly reduced.¹⁵ Nevertheless, Trx-1 can be cleaved at its C-terminal, resulting in the truncated protein, Trx-80.¹⁶ Recently, ADAM-10 and ADAM-17, two α -secretases, were found to be responsible for Trx-80 generation in brain.¹⁷ Whether, this phenomenon is ubiquitous or tissue specific is not known. It is important to note that Trx-1 and Trx-80 have contrasting roles. While Trx-1 is an oxidative stress-limiting protein with anti-inflammatory and anti-atherogenic properties, its truncated form, Trx-80, exerts pro-inflammatory effects. We recently demonstrated the ability of Trx-80 to promote differentiation of macrophages into the pro-inflammatory M1 phenotype and to accelerate atherogenic process in ApoE2.Ki mice.^{18,19}

Although these *in vitro* and *in vivo* studies are in favour of vasculoprotective effects of Trx-1 and highlight its therapeutic potential; its short half-life (<1 h) and its cleavage into Trx-80, compromise its use as a therapeutic tool in human. However, small peptides based on the active site

(W31-C-G-P-C-K36), containing the two active cysteines, have been shown to be biologically active, particularly when the amino and carboxyl terminal ends are blocked, as it facilitates their entry into cells.²⁰

In this manuscript, we have studied the effect of CB3, a Trx-1 mimetic peptide, *in vitro* and *in vivo* and we have clearly showed that it reduced oxidative stress, inflammation, and atherosclerotic lesions when used in ApoE2.Ki mice, fed high fat diet (HFD).

2. Methods

2.1 Peptide synthesis and purification

The peptide was synthesized by the platform of the 'Institut de Biologie Paris-Seine, Sorbonne Université, Paris' (for further details please see Supplementary material online).

2.2 Isolation and treatment of mouse peritoneal macrophages

As stipulated in the Annex IV of the Official Journal of the European Union (20 October 2010), for the peritoneal macrophages isolation, mice were sacrificed by cervical dislocation. Peritoneal macrophages were collected from thioglycolate-injected 12-week-old C57Bl/6 mice (Janvier labs, France) by peritoneal lavage with 10 mL of PBS, centrifuged at 1500 rpm for 10 min, and cultured in RPMI 1640 medium containing 2 mM L-glutamine and 100 U/mL Penicillin-Streptomycin (ThermoFisher Scientific, USA). Before each experiment, cells were placed in RPMI 1640 medium with 10% foetal bovine serum (FBS) for 48 h. In serum-free RPMI, cells were left untreated or were treated with LPS (10 ng/mL, *E. coli*, serotype 055: B5, Sigma-Aldrich, USA) either in the presence or in the absence of CB3 (from 0.001 to 100 μ M) or recombinant mouse Trx-1 (80 nM, IMCO, Stockholm).

2.3 Intracellular ROS measurement

Macrophages were seeded in 96-well microplates and treated with LPS (10 ng/mL) for 1 h. Thereafter, the cells were treated in the presence or absence of 80 nM Trx-1 or with various concentrations of CB3 for 1 h. After washing with PBS, cells were incubated with DCF-DA (10 μ M) at 37°C for 1 h. Finally, the cells were washed with PBS, and the fluorescence (FLU, excitation wavelength 488 nm, emission wavelength 520 nm) was measured using a fluorescent microplate reader (PerkinElmer, USA).

2.4 Extracellular H₂O₂ levels measurement

Macrophages were cultured in 96-well microplate in the presence or absence of LPS (10 ng/mL) for 4 h followed by an additional 24 h treatment by various concentrations of CB3. Extracellular H₂O₂ levels were detected with the AmplexRed reagent in combination with horseradish peroxidase (HRP) during 30 min at room temperature according to the manufacturer's instructions (Invitrogen, USA). Finally, the fluorescence (FLU, excitation wavelength 530 nm, emission wavelength 590 nm) was detected by a fluorescent microplate reader (PerkinElmer, USA).

2.5 Real-time polymerase chain reaction

Macrophages were incubated for 4 h with LPS (10 ng/mL) then in the presence or absence of CB3 (10 μ M) for 24 h in 6-well plates. Total RNA was isolated using the ReliaPrep RNA Cell Miniprep System (Promega, USA) and quantified in a NanoVue Plus spectrophotometer (GE Healthcare Life Sciences, UK). Total RNA (500 ng) was reverse-

transcribed using the RevertAid H Minus First Strand cDNA Synthesis kit (Thermo Fisher Scientific, USA) per manufacturer's instructions. mRNA expression levels of monocyte chemoattractant protein (MCP)-1, IL-1 β , IL-6, and tumor necrosis factor (TNF)- α were quantified using LightCycler 480 SYBR Green I Master (Roche, France) and normalized to 36B4 ribosomal RNA using the $\Delta\Delta C_t$ method. Primer sequences are reported in [Supplementary material online, Table S1](#).

2.6 Enzyme-linked immunosorbent assay (ELISA)

Macrophages were incubated in the presence or absence of LPS (10 ng/mL) for 4 h followed by an additional 24 h treatment with CB3 (10 μ M) in 6-well plates. MCP-1, IL-1 β , IL-6, and TNF- α cytokines released in the culture media were measured with the Mouse Elisa (Biolegend, USA). The absorbance was read at 450 nm with a microplate reader (BioTek instruments, Winooski, VT, USA).

2.7 Western blot analysis

Macrophages were treated with 10 ng/mL LPS for 4 h then with 1 μ M CB3 for 5 or 30 min in 6-well plates. Cells were scraped with lysis buffer (Sigma-Aldrich, USA) containing protease inhibitors cocktail (Roche, France) and cell lysates were incubated on ice for 1 h before centrifugation at 13 000 \times g for 10 min at 4°C. For cell fractionation procedure, see [Supplementary material online](#). Proteins content in the supernatant was determined using the bicinchoninic acid assay (BCA). Proteins (20 μ g) were separated by 12% SDS-PAGE. The resolved proteins were transferred to nitrocellulose membranes, washed and incubated with appropriate antibodies (see [Supplementary material online](#)).

2.8 ApoE2.Ki mice

All animal experiments were carried out by procedures approved by the 'Ministère de l'éducation nationale de l'enseignement supérieur et de la recherche' (01480.02, 06 September 2016) and complied with the guidelines from Directive 2010/63/EU of the European Parliament on the protection of animals used for scientific purposes. C57Bl/6.ApoE2.ki mice were obtained from Dr Nobuyo Maeda (Department of pathology and laboratory medicine, University of North Carolina) (for details see [Supplementary material online](#)). Female C57Bl/6.ApoE2.Ki mice (6 weeks old) were randomly divided into two groups ($n = 6$ per group). One group was daily injected intraperitoneally with water for 10 weeks (control, C). The other group was injected daily with CB3 (10 μ g/g of bw) for 10 weeks. This dose was chosen because in pilot experiments, (using 1, 10, and 20 CB3 μ g/g of bw), it exerted the maximum reduction of the generation of antibodies directed against oxLDL in mice plasma suggesting that the treatment HFD ApoE2.Ki mice with 10 μ g/g of bw for 10 weeks has the maximum antioxidant effect. Of note, CB3 has been already used for *in vivo* study (rats and mice) at concentrations ranged between 1 to 50 μ g/g of bw.²¹

2.9 Determination of anti-oxLDL antibodies

Human LDL ($d = 1.019\text{--}1.063$) was isolated from frozen plasma of two healthy volunteers by gradient ultracentrifugation as described previously.²² Its protein content was determined by the BCA method (Pierce, Rockford, IL, USA). Freshly prepared, filter (0.45 μ m) sterile LDL (1 mg/mL of protein in PBS), was oxidized in the presence of 10 μ M CuSO₄ for 24 h (see [Supplementary material online](#)). The use of frozen plasma is approved through the convention No. 15EFS012 between 'INSERM' and

'Etablissement Français du Sang'. The donors have given their written consent. All criteria in the convention were met.

2.10 Plasma cytokines determination

Plasma samples were separated by centrifugation of blood at 630 \times g for 20 min at 4°C and kept frozen at -80°C until required. For the quantification of adiponectin, IL-10, IL-33, and TNF- α , we used the Mouse Magnetic Luminescence screening assay (R&D Systems). Briefly, 25 μ L plasma were incubated overnight at 4°C with 25 μ L of beads linked to specific antibodies. Thereafter, 25 μ L of biotinylated antibody was added for 1 h at RT. Finally, 25 μ L of streptavidin-phycoerythrin were added for 30 min, and 150 μ L of buffer were added before reading the plate with a Luminescence 200 Millipore apparatus. Data were analysed with the xPONENT 3.1 software (Millipore, Billerica, MA, USA).

2.11 Tissue analysis by flow cytometry

Cell suspensions were obtained from spleen, bone-marrow, or peritoneal lavage of euthanized animals. Cell suspensions were incubated with monoclonal antibodies (mAbs) against surface antigens ([Supplementary material online, Table S2](#)).

2.12 Evaluation of mouse aortic lesions

At the end of the study, animals were anaesthetized and perfused transcardially with PBS before the heart and descending aortas were excised and fixed. Hearts were cut directly under and parallel to the leaflet, and the upper portions were embedded in OCT medium and frozen at -80°C until used. Sections of 10 μ m thickness were prepared from proximal aortas. The sections were stained for lipids with Oil-Red O and counterstained with Haematoxylin Harris. Ten sections, each separated by 100 μ m, were used for specific morphometric evaluation of intimal lesions. Images were captured with a CAMIRIS video camera, and the surface area covered by lesions was evaluated with ImageJ software. For localization of M1 and M2 macrophages in atherosclerotic lesions, frozen serial sections were analysed by immunohistochemistry using double immunostaining with antibodies against the macrophage marker F4/80 (Abcam, 1/500 or Santa Cruz, 1/50) and TNF- α antibody (Sigma, 1/200) or the M1 marker CD86 (Santa Cruz, 1/500) or the M2 marker CD206 (Santa Cruz, 1/500).

2.13 Statistical analysis

All values are represented as a mean \pm SEM. The difference between only two groups was analysed using non-parametric Mann-Whitney *U* test. The difference between three or more than three groups was analysed using one-way ANOVA followed by Tukey's post-test. A *P*-value <0.05 was considered to be statistically significant difference. All statistical tests were performed using the GraphPad Prism Software (V5, CA, USA).

3. Results

3.1 CB3 stability

The stability of CB3 was determined, following its incubation in mouse plasma for various periods of time (from 0 to 48 h) at 37°C, using HPLC-MS/MS. The peptide was quantified with the ratio of area peak at T₀ and every time point. The results showed a decrease of intact CB3 with time. After 24 h of incubation for example \sim 30% of CB3 was lost ([Supplementary material online, Figure S1](#)). Of note, its stability was found to be better when CB3 is dissolved in water rather than in saline

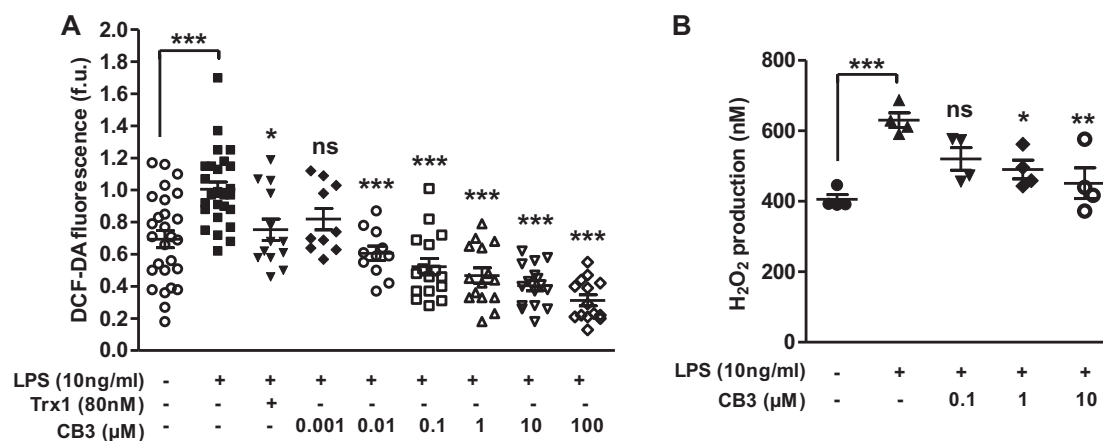


Figure 1 CB3 reduces ROS levels and H₂O₂ production in macrophages. (A) Murine macrophages were incubated with 10 ng/mL of LPS for 1 h followed by 1 h treatment with various concentrations of CB3 or with 80 nM of Trx-1. ROS levels were assessed by ROS-sensitive DCF-DA probe. Results are represented as mean \pm SEM of 10 to 27 independent experiments. (B) Murine primary macrophages were treated with 10 ng/mL LPS for 4 h followed by a 24 h treatment with various concentrations of CB3. Culture media were collected, and the H₂O₂ production was evaluated by AmplexRed probe. Results are represented as mean \pm SEM from four independent experiments. One-way ANOVA followed by Tukey's post-test was used to determine statistically significant differences as compared to LPS-treated macrophages. * $P < 0.05$; ** $P < 0.01$; *** $P < 0.001$ and ns (no statistical significance).

buffer (Supplementary material online, Figure S11). In addition, CB3 does not bind to LDL nor to HDL particles (Supplementary material online, Figure S2).

3.2 CB3 is not cytotoxic in murine macrophages

The ability of CB3 to reduce intracellular ROS levels was analysed using the DCF-DA fluorescent probe. Macrophages were treated with LPS (pro-inflammatory) and a pro-oxidative agent at 10 ng/mL (Figure 1A) in the absence or presence of Trx-1 (80 nM) or various concentrations of CB3 (0.001–100 μ M). As shown, LPS increases the ROS levels by 30%, ($P < 0.001$) compared to control macrophages. Under these pro-oxidant conditions, Trx-1 significantly decreases ROS levels by 20% ($P < 0.05$). Interestingly, in the presence of CB3 the ROS level is significantly reduced in a dose-dependent way with a maximal inhibition of about 68% ($P < 0.001$). Similarly, CB3 also reduced the extracellular levels of H₂O₂ in a dose-dependent manner (Figure 1B).

To determine whether or not the CB3 affects inflammatory processes in macrophages, we evaluated the concentrations of some major inflammatory markers such as MCP-1, IL-1 β , IL-6, and TNF- α . As shown in Figure 2, LPS significantly increased the expression of all cytokines relative to the control and the treatment of LPS-activated macrophages with CB3 significantly reduced their expression. Of note, a similar effect of CB3 on MCP-1, TNF- α expression and intracellular ROS production is also seen by human macrophages (Supplementary material online, Figure S3).

3.3 CB3 inhibits NF- κ B in murine macrophages

In order to determine the signal pathway through which CB3 exerts its anti-inflammatory effect, we explored the NF- κ B pathway; one of the major inflammatory pathways. Western blot analysis revealed that I- κ B phosphorylation (Figure 3A) was significantly increased in LPS-treated macrophages as compared to control cells (three-fold induction, $P < 0.01$). When macrophages were treated with LPS, we observed a

60% decrease in the presence of p65 in the cytoplasm ($P < 0.01$); whereas its presence was increased by 70% in the nucleus as compared to the control cells ($P < 0.01$) (Figure 3B,C). Therefore, LPS-induced I- κ B phosphorylation and p65 translocation to the nucleus, indicating the activation of the NF- κ B inflammatory pathway. In the presence of CB3, this tendency was reversed. The phosphorylation of I- κ B was rapidly and significantly decreased (two-fold inhibition) after 5 min of treatment with CB3 (Figure 3A). Figure 3B,C show that CB3 increased p65 in the cytoplasm (the level of p65 increases two-fold in the cytoplasm after 30 min of CB3 treatment as compared to LPS treatment) and decreased its translocation to the nucleus (a two-fold decrease).

3.4 CB3 does not affect total cholesterol content in murine macrophages

Macrophages were incubated with LPS (10 ng/mL) for 4 h in the presence or absence of native LDL (100 μ g protein/mL) or oxLDL (100 μ g protein/mL). The cells were then treated in the presence or absence of CB3 (10 μ M) for 24 h. During treatment, lipoproteins were not removed. Cellular total cholesterol content was determined according to the protocol described in the Methods section. The results indicated that CB3 tends to reduce the cholesterol content without however reaching a significant level (Supplementary material online, Figure S4).

3.5 Effect of CB3 on the plasma levels of oxidative and inflammatory markers in ApoE2.Ki mice fed HFD

To evaluate the antioxidant, anti-inflammatory, and vasculoprotective effects of CB3 in the pathological context of atherosclerosis, we used the ApoE2.Ki mice. This mouse model expresses the human ApoE2 isoform instead of the murine ApoE and develops atherosclerosis when fed HFD (21% of lipids).²³ Six-week-old female mice were randomized into two groups ($n = 6$ each group) and then treated daily for 10 weeks with intraperitoneal injection of water for the control group (C) or CB3 (10 μ g/g

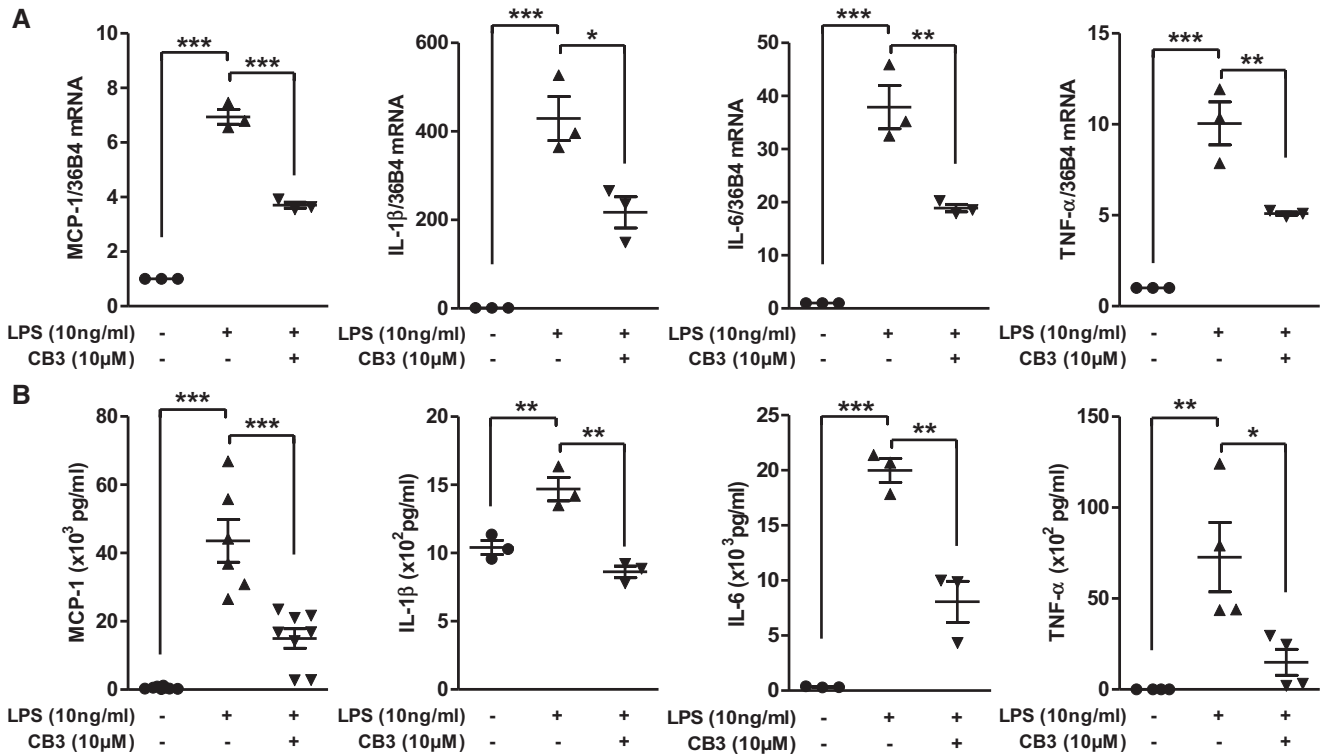


Figure 2 CB3 reduces proinflammatory cytokines mRNA and protein expression in macrophages. Murine macrophages were incubated with LPS (10 ng/ml) for 4 h followed by additional 24 h treatment with 10 μM CB3. Cell lysate and medium were collected and MCP-1, IL-1β, IL-6, TNF-α (A) mRNA and (B) protein levels were evaluated by RT-qPolymerase chain reaction and ELISA, respectively. Results are represented as mean ± SEM from 3 to 8 independent experiments. One-way ANOVA followed by Tukey's post-test was used to determine statistically significant differences as compared to LPS-treated macrophages. * $P < 0.01$, *** $P < 0.001$ and ns (no statistical significance).

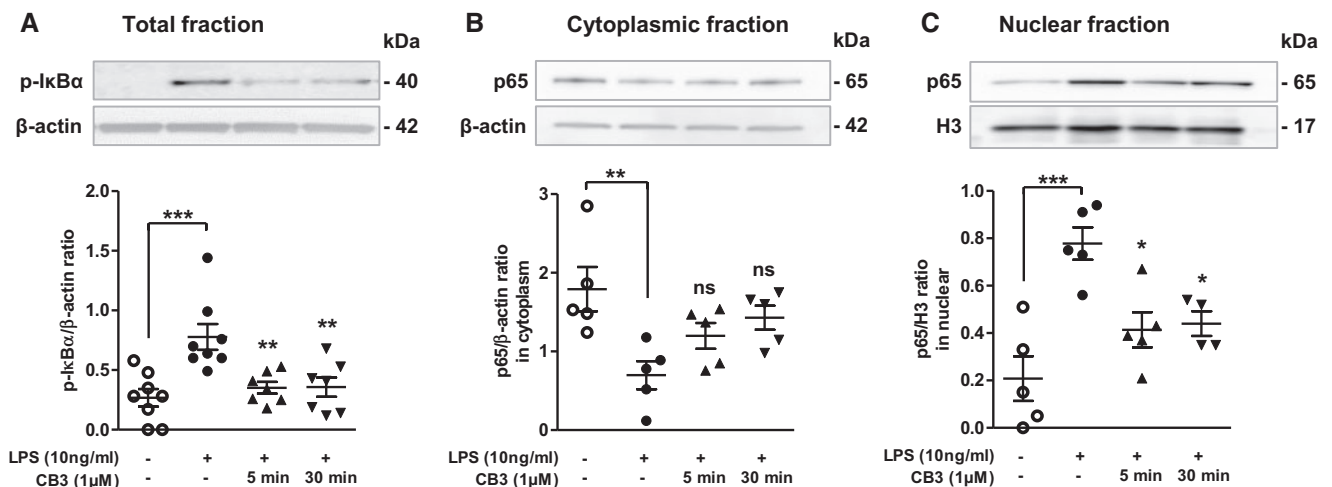


Figure 3 CB3 inhibits LPS-induced NF-κB activation in macrophages. Murine macrophages were incubated with LPS (10 ng/mL) for 4 h and then treated with 1 μM of CB3 during 5 or 30 min. 20 μg of (A) total, (B) cytoplasmic, or (C) nuclear cell lysates were separated on SDS-PAGE. The appropriate antibodies were used to visualize and quantify levels of p-IκB (p-IκB/β-actin, A) or p65 in cytoplasm (p65/β-actin, B) and in nuclei [p65/Histone3 (H3), C]. Results represent the mean ± SEM from 5 to 8 independent experiments. One-way ANOVA followed by Tukey's post-test was used to determine statistically significant differences as compared to LPS-treated macrophages. * $P < 0.05$; ** $P < 0.01$; *** $P < 0.001$ and ns (no statistical significance).

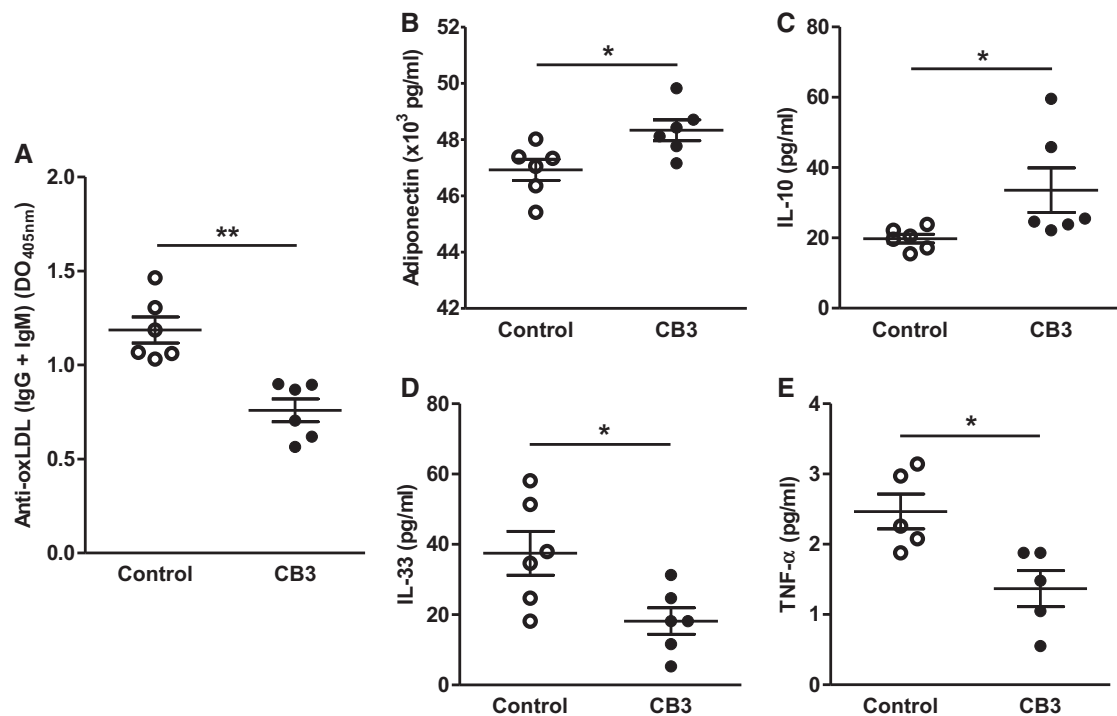


Figure 4 CB3 affects the levels of plasma oxidative and inflammatory markers in HFD-fed ApoE2.Ki. Two groups of female HFD-fed ApoE2.Ki mice were treated with CB3 (10 $\mu\text{g/g}$ bw) or with water (control) for 10 weeks. (A) Plasma levels of antibodies against oxLDL were analysed by ELISA. (B, C) Plasma anti-inflammatory cytokine levels or (D, E) pro-inflammatory cytokine levels were evaluated by the Luminex technique. Results represent the mean \pm SEM from 5 to 6 mice. Mann–Whitney’s *U* test was used to determine statistically significant differences as compared to control group. * $P < 0.05$; ** $P < 0.01$.

of bw) for the treated group (CB3). At the end of the treatment, we determined the activity of both transaminases: Aspartate aminotransferase (ASAT) and Alanine Aminotransferase (ALAT) in plasma. The result showed comparable enzymatic activities in both groups indicating that CB3 does not induce hepatic cytotoxicity. ASAT: 247.3 ± 55.1 U/L (control) vs. 206.3 ± 68.7 U/L (CB3); ALAT: 19.9 ± 4.1 U/L (control) vs. 25.4 ± 1.4 U/L (CB3). In addition, we measured body weights, food intake and total plasma cholesterol, and triglycerides of control and CB3-treated mice. The results did not show any significant differences between both groups (Supplementary material online, Figure S5). In order to demonstrate the antioxidant properties of CB3, the plasma levels of antibodies directed against oxLDL (IgG and IgM) were evaluated. Treatment of ApoE2.Ki mice fed HFD with CB3 significantly reduced the plasma concentration of anti-oxLDL antibodies by $\sim 36\%$ ($P < 0.01$) in comparison to control mice (Figure 4A). In addition, in CB3-treated mice, the levels of adiponectin and IL-10, two factors known to exert an anti-inflammatory effect, are significantly increased in the plasma in comparison to control mice (Figure 4B and C). In contrast, the plasma levels of TNF- α and IL-33, which are involved in inflammation, decreased significantly in the CB3-treated mice in comparison to the control group (Figure 4D and E).

3.6 CB3 reduces the abundance of activated macrophages in HFD ApoE2.Ki mice

To evaluate the global impact of systemic administration of CB3 on the haematopoietic compartment and resident macrophages in ApoE2.Ki

mice fed HFD, we performed multiparametric flow cytometry analysis on the spleen of treated animals as compared to control mice. While long-term CB3 treatment had no measurable effect on cells belonging to the adaptive compartment of the immune system (data not shown), only resident macrophages were significantly affected, as CB3 treatment reduces the percentages of activated macrophages by 32.43% amongst the total CD45+ cell compartment (CB3 1.09 ± 0.09 vs C 1.61 ± 0.14) (Figure 5).

3.7 CB3 exerts an anti-atherogenic effect in ApoE2.Ki mice

Consistent with the findings of Sullivan *et al.*,²³ we observed a significant increase of the lesion size in HFD-challenged ApoE2.Ki mice as compared to ApoE2.Ki mice, fed on a regular chow diet. Therefore, we evaluated the mean lesion area in proximal aortas of control and CB3-treated groups. The results, shown in Figure 6A, indicate a significant decrease ($\sim 36\%$, $P < 0.05$) in lesion area of CB3-treated mice vs. the control group. In addition, lesional macrophages in control mice express high levels of CD86 and low levels of CD206, suggesting the predominant presence of proinflammatory M1 macrophages. However, when ApoE2.Ki mice were treated with CB3, the number of total macrophages (F4/80+) was reduced (Supplementary material online, Figure S6) among which M1 macrophages (CD86+) or (TNF- α +) were significantly reduced respectively (7.02 ± 0.37 for control vs 3.76 ± 0.47 for CB3-treated mice, $P < 0.01$) and (5.83 ± 0.87 for control vs 1.16 ± 0.40 for

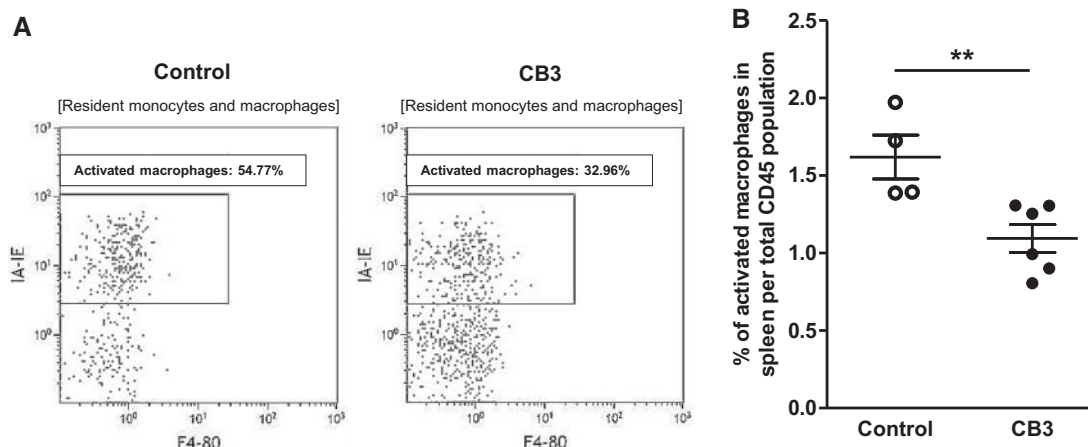


Figure 5 CB3 reduces activated macrophages in ApoE2.Ki mice fed HFD. Two groups of female HFD-fed ApoE2.Ki mice were treated with CB3 (10 µg/g bw) or with water (control) for 10 weeks. Number of activated macrophages in the spleen were determined by multiparametric flow cytometry analysis and normalized per total CD45⁺ population (Supplementary material online). (A) A representative dot-plot of activated macrophages is shown. (B) Percentages of activated macrophages among total CD45⁺ population in untreated (C) and CB3-treated (CB3) animals. Results represent the mean ± SEM from 4 to 6 mice. Mann–Whitney’s *U* test was used to determine statistically significant differences as compared to control group. ***P* < 0.01.

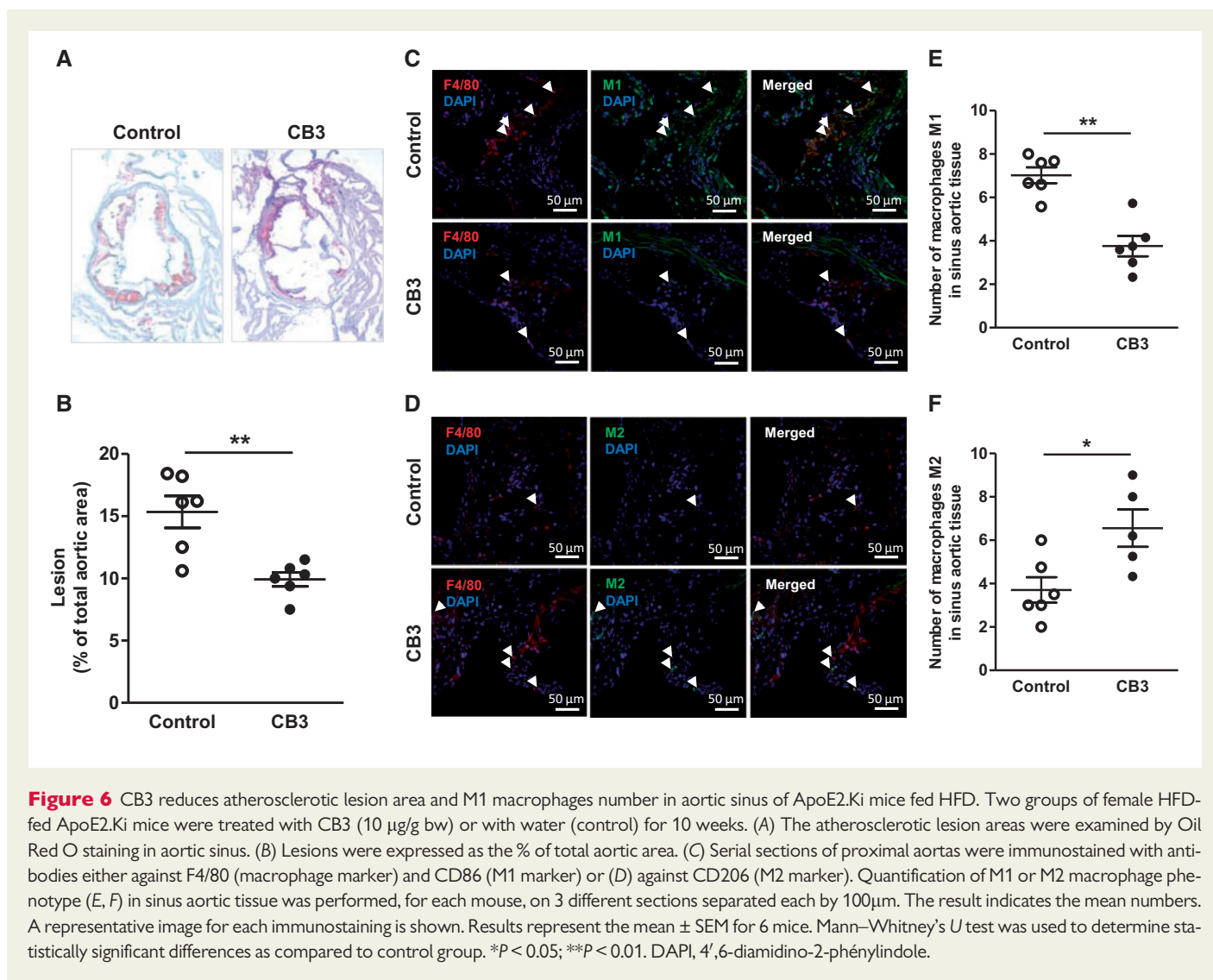
CB3-treated mice, *P* < 0.01). The number of M2 macrophages (CD206⁺) was, in contrast, significantly increased (3.71 ± 0.59 for control vs. 6.56 ± 0.86 for CB3-treated mice, *P* < 0.05) (Figure 6B and Supplementary material online, Figure S7).

4. Discussion

We conducted the present study using CB3, a Trx-1-mimetic peptide, based on the active site Cys³²-Gly-Pro-Cys³⁵ (CXXC) of Trx-1, as alternative approach to the use of Trx-1 in therapy. This approach has been taken because full length Trx-1 can be cleaved leading to generation of proatherogenic Trx-80 particles which can compromise its potential therapeutic use in CVD. We showed that CB3 was able to reduce, in a dose-dependent manner, the level of intracellular ROS (Figure 1A) and extracellular H₂O₂ (Figure 1B) generated in LPS-activated macrophages. In addition, CB3 significantly decreased the level of potent pro-inflammatory cytokines, like MCP-1, IL-1β, IL-6, and TNF-α, in LPS-activated macrophages (Figure 2) through the inhibition of the NF-κB pathway (Figure 3). Of note, it is well established that ROS are directly induced, as second messengers, in the activation of NF-κB by the oxidation of a cysteine-SH group. Reduction of ROS levels could, at least in part, represent the underlying molecular mechanism by which CB3 acts to inhibit NF-κB pathway and to reduce inflammation. Moreover, intraperitoneal injection of CB3 peptide into HFD-fed ApoE2.Ki mice reduced the levels of circulating antibodies directed against oxLDL reflecting its anti-oxidative activity (Figure 4A) without affecting the plasma levels of total cholesterol or triglycerides (Supplementary material online, Figure S5C and D). CB3 treatment significantly increased anti-inflammatory proteins such as adiponectin and IL-10 (Figure 4B and C) and significantly reduced plasma levels of pro-inflammatory factors like IL-33 and TNF-α (Figure 4D and E). It also reduced the number of activated macrophages (M1 phenotype) in the spleen (Figure 5) and in the arterial lesion area (Figure 6B) suggesting its ability to orient macrophages toward the M2 anti-inflammatory phenotype. Finally, treatment of HFD-fed ApoE2.Ki mice

with CB3 significantly reduced the aortic lesion surface area (Figure 6A). Taken together, our results indicate that CB3 exerts several protective effects and could represent a novel therapeutic approach to treat CVDs.

During the last decades, tremendous efforts have been made to study the role of certain major risk factors such as hypertension, hyperglycaemia and hypercholesterolaemia in the development of CVD. This strategy allowed the generation of a first set of medications which are currently in use such as angiotensin-converting enzyme inhibitors (ACEIs), angiotensin II receptor blockers (ARBs), anticoagulants, cholesterol-lowering drugs (statins), beta-blockers, and some anti-inflammatory medicines (NSAID, glucocorticoids).²⁴ Although, many of these drugs have shown efficacy; many exert also a variety of undesirable effects and therefore are not suitable to use for a long-term treatment.^{25–27} Therefore, new medications to treat CVD are required. Given the adverse side effects associated with pharmacological therapy, therapeutics based on synthetic peptides have become an alternative strategy in the prevention of CVD. The advanced technologies which now allow the generation of stable, specific and efficient peptides, and peptidomimetics, has increased dramatically the interest for their use as potential therapeutic agents.^{28,29} For example, different apolipoprotein-AI (apoA-I) mimetic peptides such as the 4F,³⁰ D-4F, and L-4F,³¹ 6F,³² the FAMP, which has been reported to function specifically via ABCA1 (ATP-binding Cassette transporter A1),³³ and 5A³⁴ were generated. These peptides demonstrated atheroprotective effects in apoE^{-/-} mice, and 5A is under consideration for clinical trials.³⁵ Similarly, several mimetic peptides based on apoE structure have also been developed (reviewed by reference 24) The most studied peptide is the Ac-hE18A-NH₂, composed by a region of the LDL binding domain of apoE linked to the 18A apoA-I mimetic peptide.³⁶ This peptide reduced plasma cholesterol and atheroma formation and improved endothelial function.^{37,38} Moreover, It is important to note that a large collection of peptides of varying lengths have been reported for several biomedical applications, including diagnosis and therapy for atherosclerosis.³⁹ Although, an increasing number of studies have been using nanoparticle-associated



therapeutic peptides for atherosclerosis, some studies did not associate nanoparticle such as the D-4F, apoA-I mimetic peptide, which was given orally to apoE^{-/-} mice⁴⁰ or CB3 peptide which was intraperitoneally infused (present study).

Although lipid disorder is a major risk factor for CVD which justify the use of apoA-I or apoE mimetic peptides, inflammation, whether is related to lipid disorders or not, is generally accepted to participate in atherosclerosis progression.⁴¹ Therefore, targeting macrophages as a major actor of inflammation and proteins involving in chronic inflammation can also be an interesting therapeutic strategy for CVD treatment. Thus for example, certain mimetic peptides for Suppressors of Cytokine Signalling (SOCS) reduced inflammatory and exert atheroprotective roles.^{42,43} In our present study, the use of Trx-1-mimetic peptide, CB3, is of great importance as it reduced oxidative stress, inflammation, and atherosclerotic lesions in ApoE2.Ki mice fed HFD without affecting lipid profile. Our results are strengthened by previous data indicating that small peptides based on the Trx-1 active site (W31-C-G-P-C-K36), containing the two active cysteines, were biologically active, particularly when the amino and carboxy terminal ends were blocked which facilitates their entry into cells,²⁰ Such peptides displayed a higher efficiency, compared to traditional antioxidant agents, such as N-acetylcysteine (NAC), dithiothreitol (DTT), glutathione (GSH), and ascorbic acid, in a variety of cellular pathways.^{20,44}

Aging and other risk factors can induce oxidative stress, particularly in vessels, where ROS contribute to vascular disease.⁴⁵ ROS in the vascular wall are generated by NADPH oxidases (NOX), xanthine oxidase, mitochondria, and dysfunctional endothelial nitric oxide synthase (eNOS). NOX2, expressed by endothelial cells and macrophages, is a major producer of O₂⁻ and disruption of its gene reduces atherogenesis in ApoE^{-/-} mice.⁴⁶ The early stage of atherosclerosis is associated with high levels of peroxide anion (O₂⁻) in human, rabbit, and primate models.⁴⁷ A major atherogenic mechanism occurs via the O₂⁻-mediated inactivation of nitric oxide (NO) leading to, not only peroxynitrite (ONOO⁻) formation but also to loss of vasculoprotective effects of NO. Through its powerful oxidizing properties, ONOO⁻ causes irreversible damage to proteins, lipids, and DNA.^{45,47,48} In addition, O₂⁻ is the precursor of H₂O₂ that can spontaneously convert to hydroxyl radical (OH[•]). Due to its extreme reactivity, OH[•] can damage most cellular compartments and contribute, with H₂O₂, to LDL oxidation in vessel wall.^{45,47} In addition, H₂O₂ reacts with myeloperoxidase, particularly in immune cells, to form highly reactive hypochlorous acid (HOCl). It was recently demonstrated that high concentration of H₂O₂ causes phenotypical transition of fibroblasts and smooth muscle cells in atherosclerotic plaques related to human advanced phenotype and instable plaque.⁴⁵ The biological impact of ROS depends not only on their quantities but also on their chemical nature,

subcellular and tissue location, and the rates of their formation and degradation. Otherwise, increased ROS favour pro-inflammatory genes expression via redox-sensitive transcription factor like NF- κ B. Our results demonstrate a potent anti-oxidative effect of CB3 that act probably by scavenging H₂O₂. This mechanism could, at least in part, indirectly explain the anti-inflammatory role of CB3.

Hence, the CXXC peptide is effectively protecting against oxidative stress and inflammation and could represent a new class of compounds for preventing and/or treating CVD. The CB3 peptide could be particularly useful in old people who have a high risk to develop CVD due, at least in part, to the increased cleavage of Trx-1 and the loss of its vasculoprotective effects.¹⁹

Supplementary material

Supplementary material is available at *Cardiovascular Research* online.

Acknowledgements

We thank Dr Christophe Piesse for synthesis of Trx-1 mimetic peptide (Peptide synthesis Platform, IBPS-Paris), Dr Nadir Benslimane and Julie Knoertzer for their precious help with mice housing and treatments (Animal house platform, IBPS-Paris), and Raphaël Thuillet for the immunohistochemical studies and Dr Christine Balducci Biophytis-Paris, for peptide stability analysis.

Conflict of interest: none declared.

Funding

This work was supported by the 'Fondation Coeur et Artères' [FCA14T4] and the 'Institut de Biologie Paris-Seine' for the 'Action incitative' program.

References

- Benjamin EJ, Blaha MJ, Chiuve SE, Cushman M, Das SR, Deo R, de Ferranti SD, Floyd J, Fornage M, Gillespie C, Isasi CR, Jimenez MC, Judd SE, Lackland D, Lichtman JH, Lisabeth L, Liu S, Longenecker CT, Mackey RH, Matsushita K, Mozaffarian D, Mussolino ME, Nasir K, Neumar RW, Palaniappan L, Pandey DK, Thiagarajan RR, Reeves MJ, Ritchey M, Rodriguez CJ, Roth GA, Rosamond WD, Sasson C, Towfighi A, Tsao CW, Turner MB, Virani SS, Voeks JH, Willey JZ, Wilkins JT, Wu JH, Alger HM, Wong SS, Muntner P. Heart disease and stroke statistics-2017 update: a report from the American Heart Association. *Circulation* 2017;**135**: e146–e603.
- Libby P. Inflammation in atherosclerosis. *Nature* 2002;**420**:868–874.
- Cochain C, Zernecke A. Macrophages in vascular inflammation and atherosclerosis. *Pflugers Arch* 2017;**469**:485–499.
- Ginhoux F, Schultze JL, Murray PJ, Ochando J, Biswas SK. New insights into the multi-dimensional concept of macrophage ontogeny, activation and function. *Nat Immunol* 2016;**17**:34–40.
- Mills CD, Kincaid K, Alt JM, Heilman MJ, Hill AM. M-1/M-2 macrophages and the Th1/Th2 paradigm. *J Immunol* 2000;**164**:6166–6173.
- Gordon S. Alternative activation of macrophages. *Nat Rev Immunol* 2003;**3**:23–35.
- Mantovani A, Sica A, Sozzani S, Allavena P, Vecchi A, Locati M. The chemokine system in diverse forms of macrophage activation and polarization. *Trends Immunol* 2004;**25**:677–686.
- Montecucco F, Liberale L, Bonaventura A, Vecchie A, Dallegri F, Carbone F. The role of inflammation in cardiovascular outcome. *Curr Atheroscler Rep* 2017;**19**:11.
- Bouhrel MA, Derudas B, Rigamonti E, Dievart R, Brozek J, Haulon S, Zawadzki C, Jude B, Torpiger G, Marx N, Staels B, Chinetti-Gbaguidi G. PPARgamma activation primes human monocytes into alternative M2 macrophages with anti-inflammatory properties. *Cell Metab* 2007;**6**:137–143.
- Ohashi K, Parker JL, Ouchi N, Higuchi A, Vita JA, Gokce N, Pedersen AA, Kalthoff C, Tullin S, Sams A, Summer R, Walsh K. Adiponectin promotes macrophage polarization toward an anti-inflammatory phenotype. *J Biol Chem* 2010;**285**:6153–6160.
- Madamanchi NR, Vendrov A, Runge MS. Oxidative stress and vascular disease. *Arterioscler Thromb Vasc Biol* 2005;**25**:29–38.

- Mahmood DF, Abderrazak A, El Hadri K, Simmet T, Rouis M. The thioredoxin system as a therapeutic target in human health and disease. *Antioxid Redox Signal* 2013;**19**:1266–1303.
- Mitsui A, Hamuro J, Nakamura H, Kondo N, Hirabayashi Y, Ishizaki-Koizumi S, Hirakawa T, Inoue T, Yodoi J. Overexpression of human thioredoxin in transgenic mice controls oxidative stress and life span. *Antioxid Redox Signal* 2002;**4**:693–696.
- Hattori I, Takagi Y, Nakamura H, Nozaki K, Bai J, Kondo N, Sugino T, Nishimura M, Hashimoto N, Yodoi J. Intravenous administration of thioredoxin decreases brain damage following transient focal cerebral ischemia in mice. *Antioxid Redox Signal* 2004;**6**:81–87.
- Hadri KE, Mahmood DFD, Couchie D, Jguirim-Souissi I, Genze F, Diderot V, Syrovets T, Lunov O, Simmet T, Rouis M. Thioredoxin-1 promotes anti-inflammatory macrophages of the M2 phenotype and antagonizes atherosclerosis. *Arterioscler Thromb Vasc Biol* 2012;**32**:1445–1452.
- Pekkarı K, Holmgren A. Truncated thioredoxin: physiological functions and mechanism. *Antioxid Redox Signal* 2004;**6**:53–61.
- Gil-Bea F, Akterin S, Persson T, Mateos L, Sandebring A, Avila-Cariño J, Gutierrez-Rodriguez A, Sundström E, Holmgren A, Winblad B, Cedazo-Minguez A. Thioredoxin-80 is a product of alpha-secretase cleavage that inhibits amyloid-beta aggregation and is decreased in Alzheimer's disease brain. *EMBO Mol Med* 2012;**4**:1097–1111.
- Mahmood DF, Abderrazak A, Couchie D, Lunov O, Diderot V, Syrovets T, Slimane MN, Gosselet F, Simmet T, Rouis M, El Hadri K. Truncated thioredoxin (Trx-80) promotes pro-inflammatory macrophages of the M1 phenotype and enhances atherosclerosis. *J Cell Physiol* 2013;**228**:1577–1583.
- Couchie D, Vaisman B, Abderrazak A, Mahmood DFD, Hamza MM, Canesi F, Diderot V, El Hadri K, Negre-Salvayre A, Le Page A, Fulop T, Remaley AT, Rouis M. Human plasma thioredoxin-80 increases with age and in ApoE-/- mice induces inflammation, angiogenesis, and atherosclerosis. *Circulation* 2017;**136**:464–475.
- Bachnoff N, Trus M, Atlas D. Alleviation of oxidative stress by potent and selective thioredoxin-mimetic peptides. *Free Radic Biol Med* 2011;**50**:1355–1367.
- Cohen-Kutner M, Khomsky L, Trus M, Aisner Y, Niv MY, Benhar M, Atlas D. Thioredoxin-mimetic peptides (TXM) reverse auranofin induced apoptosis and restore insulin secretion in insulinoma cells. *Biochem Pharmacol* 2013;**85**:977–990.
- Santanam N, Parthasarathy S. Paradoxical actions of antioxidants in the oxidation of low density lipoprotein by peroxidases. *J Clin Invest* 1995;**95**:2594–2600.
- Sullivan PM, Mezdour H, Quarfordt SH, Maeda N. Type III hyperlipoproteinemia and spontaneous atherosclerosis in mice resulting from gene replacement of mouse Apoe with human Apoe*2. *J Clin Invest* 1998;**102**:130–135.
- Recio C, Maione F, Iqbal AJ, Mascolo N, De Feo V. The potential therapeutic application of peptides and peptidomimetics in cardiovascular disease. *Front Pharmacol* 2017;**7**:526.
- Costopoulos C, Niespialowska-Studen M, Kukreja N, Gorog DA. Novel oral anticoagulants in acute coronary syndrome. *Int J Cardiol* 2013;**167**:2449–2455.
- Cheng J, Zhang W, Zhang X, Han F, Li X, He X, Li Q, Chen J. Effect of angiotensin-converting enzyme inhibitors and angiotensin II receptor blockers on all-cause mortality, cardiovascular deaths, and cardiovascular events in patients with diabetes mellitus: a meta-analysis. *JAMA Intern Med* 2014;**174**:773–785.
- Stein EA, Raal FJ. Lipid-lowering drug therapy for CVD prevention: looking into the future. *Curr Cardiol Rep* 2015;**17**:104.
- Goodwin D, Simerska P, Toth I. Peptides as therapeutics with enhanced bioactivity. *Curr Med Chem* 2012;**19**:4451–4461.
- Fosgerau K, Hoffmann T. Peptide therapeutics: current status and future directions. *Drug Discov Today* 2015;**20**:122–128.
- Navab M, Anantharamaiah GM, Reddy ST, Hama S, Hough G, Grijalva VR, Yu N, Ansell BJ, Datta G, Garber DW, Fogelman AM. Apolipoprotein A-I mimetic peptides. *Arterioscler Thromb Vasc Biol* 2005;**25**:1325–1331.
- Navab M, Anantharamaiah GM, Hama S, Garber DW, Chaddha M, Hough G, Lallone R, Fogelman AM. Oral administration of an Apo A-I mimetic Peptide synthesized from D-amino acids dramatically reduces atherosclerosis in mice independent of plasma cholesterol. *Circulation* 2002;**105**:290–292.
- Navab M, Hough G, Buga GM, Su F, Wagner AC, Meriwether D, Chattopadhyay A, Gao F, Grijalva V, Danciger JS, Van Lenten BJ, Org E, Lusis AJ, Pan C, Anantharamaiah GM, Farias-Eisner R, Smyth SS, Reddy ST, Fogelman AM. Transgenic 6F tomatoes act on the small intestine to prevent systemic inflammation and dyslipidemia caused by Western diet and intestinally derived lysophosphatidic acid. *J Lipid Res* 2013;**54**:3403–3418.
- Uehara Y, Ando S, Yahiro E, Oniki K, Ayaori M, Abe S, Kawachi E, Zhang B, Shioi S, Tanigawa H, Imaizumi S, Miura S, Saku K. FAMP, a novel apoA-I mimetic peptide, suppresses aortic plaque formation through promotion of biological HDL function in ApoE-deficient mice. *J Am Heart Assoc* 2013;**2**:e000048.
- Remaley AT, Thomas F, Stonik JA, Demosky SJ, Bark SE, Neufeld EB, Bocharov AV, Vishnyakova TG, Patterson AP, Eggerman TL, Santamarina-Fojo S, Brewer HB. Synthetic amphipathic helical peptides promote lipid efflux from cells by an ABCA1-dependent and an ABCA1-independent pathway. *J Lipid Res* 2003;**44**:828–836.
- Amar MJ, D'Souza W, Turner S, Demosky S, Sviridov D, Stonik J, Luchoomun J, Voogt J, Hellerstein M, Sviridov D, Remaley AT. 5A apolipoprotein mimetic peptide promotes cholesterol efflux and reduces atherosclerosis in mice. *J Pharmacol Ther* 2010;**334**:634–641.
- Sharifov OF, Nayyar G, Garber DW, Handattu SP, Mishra VK, Goldberg D, Anantharamaiah GM, Gupta H. Apolipoprotein E mimetics and cholesterol-lowering properties. *Am J Cardiovasc Drugs* 2011;**11**:371–381.

37. Gupta H, White CR, Handattu S, Garber DW, Datta G, Chaddha M, Dai L, Gianturco SH, Bradley WA, Anantharamaiah GM. Apolipoprotein E mimetic peptide dramatically lowers plasma cholesterol and restores endothelial function in watanabe heritable hyperlipidemic rabbits. *Circulation* 2005;**111**:3112–3118.
38. Datta G, White CR, Dashti N, Chaddha M, Palgunachari MN, Gupta H, Handattu SP, Garber DW, Anantharamaiah GM. Anti-inflammatory and recycling properties of an apolipoprotein mimetic peptide, Ac-hE18A-NH(2). *Atherosclerosis* 2010;**208**:134–141.
39. Chung EJ. Targeting and therapeutic peptides in nanomedicine for atherosclerosis. *Exp Biol Med (Maywood)* 2016;**241**:891–898.
40. Navab M, Anantharamaiah GM, Reddy ST, Hama S, Hough G, Grijalva VR, Wagner AC, Frank JS, Datta G, Garber D, Fogelman AM. Oral D-4F causes formation of pre-beta high-density lipoprotein and improves high-density lipoprotein-mediated cholesterol efflux and reverse cholesterol transport from macrophages in apolipoprotein E-null mice. *Circulation* 2004;**109**:3215–3220.
41. Libby P, Ridker PM, Hansson GK. Progress and challenges in translating the biology of atherosclerosis. *Nature* 2011;**473**:317–325.
42. Mujtaba MG, Flowers LO, Patel CB, Patel RA, Haider MI, Johnson HM. Treatment of mice with the suppressor of cytokine signaling-1 mimetic peptide, tyrosine kinase inhibitor peptide, prevents development of the acute form of experimental allergic encephalomyelitis and induces stable remission in the chronic relapsing/remitting form. *J Immunol* 2005;**175**:5077–5086.
43. Ahmed CMI, Larkin J, Johnson HM. SOCS1 mimetics and antagonists: a complementary approach to positive and negative regulation of immune function. *Front Immunol* 2015;**6**:183.
44. Kim SR, Lee KS, Park SJ, Min KH, Lee MH, Lee KA, Bartov O, Atlas D, Lee YC. A novel dithiol amide CB3 attenuates allergic airway disease through negative regulation of p38 mitogen-activated protein kinase. *Am J Respir Crit Care Med* 2011; **183**:1015–1024.
45. Munzel T, Camici GG, Maack C, Bonetti NR, Fuster V, Kovacic JC. Impact of oxidative stress on the heart and vasculature: Part 2 of a 3-part series. *J Am Coll Cardiol* 2017;**70**:212–229.
46. Barry-Lane PA, Patterson C, van der Merwe M, Hu Z, Holland SM, Yeh ET, Runge MS. p47phox is required for atherosclerotic lesion progression in ApoE(-/-) mice. *J Clin Invest* 2001;**108**:1513–1522.
47. Stocker R, Keaney JF Jr. Role of oxidative modifications in atherosclerosis. *Physiol Rev* 2004;**84**:1381–1478.
48. Drummond GR, Sobey CG. Endothelial NADPH oxidases: which NOX to target in vascular disease? *Trends Endocrinol Metab* 2014;**25**:452–463.